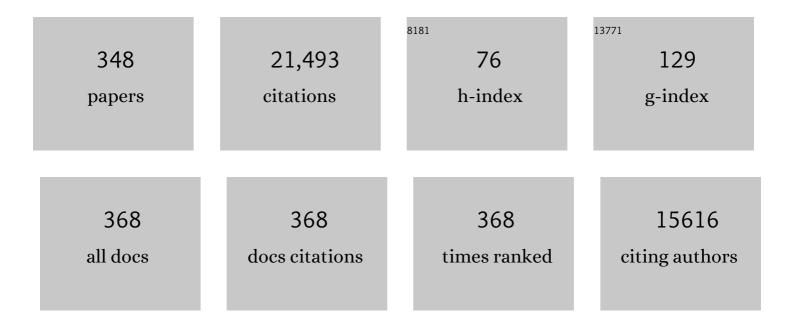
List of Publications by Year in descending order

Source: https://exaly.com/author-pdf/3040510/publications.pdf Version: 2024-02-01



#	Article	IF	CITATIONS
1	A Luminescent Microporous Metal–Organic Framework for the Fast and Reversible Detection of High Explosives. Angewandte Chemie - International Edition, 2009, 48, 2334-2338.	13.8	1,168
2	Metal–organic frameworks based on flexible ligands (FL-MOFs): structures and applications. Chemical Society Reviews, 2014, 43, 5867-5895.	38.1	739
3	Highly graphitized nitrogen-doped porous carbon nanopolyhedra derived from ZIF-8 nanocrystals as efficient electrocatalysts for oxygen reduction reactions. Nanoscale, 2014, 6, 6590-6602.	5.6	720
4	Stabilizing Cesium Lead Halide Perovskite Lattice through Mn(II) Substitution for Air-Stable Light-Emitting Diodes. Journal of the American Chemical Society, 2017, 139, 11443-11450.	13.7	705
5	Beryllium-free Li4Sr(BO3)2 for deep-ultraviolet nonlinear optical applications. Nature Communications, 2014, 5, 4019.	12.8	384
6	Deep-Ultraviolet Transparent Phosphates RbBa <sub>2</sub> (PO <sub>3</sub> ) <sub>5</sub> and Rb <sub>2</sub> Ba <sub>3</sub> (P <sub>2</sub> O <sub>7</sub> ) <sub>2</sub> Show Nonlinear Optical Activity from Condensation of [PO <sub>4</sub> ] <sup>3–</sup> Units. Journal of the American Chemical Society, 2014, 136, 8560-8563.	13.7	297
7	A Silver(I) Coordination Polymer Chain Containing Nanosized Tubes with Anionic and Solvent Molecule Guests. Angewandte Chemie - International Edition, 2000, 39, 2468-2470.	13.8	295
8	A porous metal-organic framework with ultrahigh acetylene uptake capacity under ambient conditions. Nature Communications, 2015, 6, 7575.	12.8	288
9	Carbon dioxide capture and conversion by an acid-base resistant metal-organic framework. Nature Communications, 2017, 8, 1233.	12.8	286
10	Controllable Coordination-Driven Self-Assembly: From Discrete Metallocages to Infinite Cage-Based Frameworks. Accounts of Chemical Research, 2015, 48, 201-210.	15.6	276
11	Beryllium-Free Rb <sub>3</sub> Al <sub>3</sub> B <sub>3</sub> O <sub>10</sub> F with Reinforced Interlayer Bonding as a Deep-Ultraviolet Nonlinear Optical Crystal. Journal of the American Chemical Society, 2015, 137, 2207-2210.	13.7	237
12	Two-Dimensional Hybrid Perovskite-Type Ferroelectric for Highly Polarization-Sensitive Shortwave Photodetection. Journal of the American Chemical Society, 2019, 141, 2623-2629.	13.7	237
13	Tailored Engineering of an Unusual (C <sub>4</sub> H <sub>9</sub> NH <sub>3</sub> ) <sub>2</sub> (CH <sub>3</sub> NH <sub>3</sub> ) <sub>2&lt; Twoâ€Dimensional Multilayered Perovskite Ferroelectric for a Highâ€Performance Photodetector. Angewandte Chemie - International Edition. 2017. 56. 12150-12154.</sub>	/sub>Pb <s 13.8</s 	ub>31
14	Designing a Beryllium-Free Deep-Ultraviolet Nonlinear Optical Material without a Structural Instability Problem. Journal of the American Chemical Society, 2016, 138, 2961-2964.	13.7	220
15	A Nanometer-Sized Metallosupramolecular Cube withOhSymmetry. Journal of the American Chemical Society, 2000, 122, 4819-4820.	13.7	215
16	Enhancing CO2 electrolysis through synergistic control of non-stoichiometry and doping to tune cathode surface structures. Nature Communications, 2017, 8, 14785.	12.8	215
17	Tailored Synthesis of a Nonlinear Optical Phosphate with a Short Absorption Edge. Angewandte Chemie - International Edition, 2015, 54, 4217-4221.	13.8	205
18	A multi-metal-cluster MOF with Cu4I4 and Cu6S6 as functional groups exhibiting dual emission with both thermochromic and near-IR character. Chemical Science, 2013, 4, 1484.	7.4	202

#	Article	IF	CITATIONS
19	Non-Centrosymmetric RbNaMgP <sub>2</sub> O <sub>7</sub> with Unprecedented Thermo-Induced Enhancement of Second Harmonic Generation. Journal of the American Chemical Society, 2018, 140, 1592-1595.	13.7	200
20	Bilayered Hybrid Perovskite Ferroelectric with Giant Two-Photon Absorption. Journal of the American Chemical Society, 2018, 140, 6806-6809.	13.7	185
21	Two Non-Ï€-Conjugated Deep-UV Nonlinear Optical Sulfates. Journal of the American Chemical Society, 2019, 141, 3833-3837.	13.7	183
22	Inorganicâ^'Organic Hybrid Coordination Polymers:Â A New Frontier for Materials Research. Crystal Growth and Design, 2007, 7, 10-14.	3.0	182
23	Hydrothermal syntheses, structures and properties of terephthalate-bridged polymeric complexes with zig-zag chain and channel structures. Dalton Transactions RSC, 2001, , 2335-2340.	2.3	180
24	A Photoferroelectric Perovskiteâ€Type Organometallic Halide with Exceptional Anisotropy of Bulk Photovoltaic Effects. Angewandte Chemie - International Edition, 2016, 55, 6545-6550.	13.8	175
25	Two polymeric 36-metal pure lanthanide nanosize clusters. Chemical Science, 2013, 4, 3104.	7.4	154
26	Control the Structure of Zr-Tetracarboxylate Frameworks through Steric Tuning. Journal of the American Chemical Society, 2017, 139, 16939-16945.	13.7	153
27	Highly selective carbon dioxide adsorption in a water-stable indium–organic framework material. Chemical Communications, 2012, 48, 9696.	4.1	148
28	Inchâ€Size Single Crystal of a Leadâ€Free Organic–Inorganic Hybrid Perovskite for Highâ€Performance Photodetector. Advanced Functional Materials, 2018, 28, 1705467.	14.9	146
29	Copperâ€Catalyzed Intermolecular Amination of Acidic Aryl CH Bonds with Primary Aromatic Amines. Advanced Synthesis and Catalysis, 2010, 352, 1301-1306.	4.3	145
30	An Unprecedented Biaxial Trilayered Hybrid Perovskite Ferroelectric with Directionally Tunable Photovoltaic Effects. Journal of the American Chemical Society, 2019, 141, 7693-7697.	13.7	145
31	Chiral Leadâ€Free Hybrid Perovskites for Selfâ€Powered Circularly Polarized Light Detection. Angewandte Chemie - International Edition, 2021, 60, 8415-8418.	13.8	144
32	An Unprecedented Antimony(III) Borate with Strong Linear and Nonlinear Optical Responses. Angewandte Chemie - International Edition, 2020, 59, 7793-7796.	13.8	143
33	Solidâ€State Reversible Quadratic Nonlinear Optical Molecular Switch with an Exceptionally Large Contrast. Advanced Materials, 2013, 25, 4159-4163.	21.0	136
34	In situ large-scale construction of sulfur-functionalized metal–organic framework and its efficient removal of Hg( <scp>ii</scp> ) from water. Journal of Materials Chemistry A, 2016, 4, 15370-15374.	10.3	135
35	Alloying <i>n</i> â€Butylamine into CsPbBr <sub>3</sub> To Give a Twoâ€Dimensional Bilayered Perovskite Ferroelectric Material. Angewandte Chemie - International Edition, 2018, 57, 8140-8143.	13.8	135
36	The First 2D Hybrid Perovskite Ferroelectric Showing Broadband Whiteâ€Light Emission with High Color Rendering Index. Advanced Functional Materials, 2019, 29, 1805038.	14.9	134

#	Article	IF	CITATIONS
37	Distinct Molecular Motions in a Switchable Chromophore Dielectric 4â€ <i>N</i> , <i>N</i> ,â€Dimethylaminoâ€4′â€ <i>N</i> ′â€methylstilbazolium Trifluoromethanesulfonate. Functional Materials, 2012, 22, 4855-4861.	Adv <b>æne</b> ed	133
38	A regenerative metal–organic framework for reversible uptake of Cd( <scp>ii</scp> ): from effective adsorption to in situ detection. Chemical Science, 2016, 7, 5983-5988.	7.4	133
39	Truncated octahedral coordination cage incorporating six tetranuclear-metal building blocks and twelve linear edges. Chemical Science, 2012, 3, 2321.	7.4	131
40	Effective visible-light driven CO <sub>2</sub> photoreduction via a promising bifunctional iridium coordination polymer. Chemical Science, 2014, 5, 3808.	7.4	131
41	Deep-Ultraviolet Transparent Cs <sub>2</sub> LiPO <sub>4</sub> Exhibits an Unprecedented Second Harmonic Generation. Chemistry of Materials, 2016, 28, 7110-7116.	6.7	130
42	Synthesis, Crystal Structure and Fluorescence of Two Novel Mixed-Ligand Cadmium Coordination Polymers with Different Structural Motifs. European Journal of Inorganic Chemistry, 2003, 2003, 2705-2710.	2.0	128
43	Exploring a Leadâ€free Semiconducting Hybrid Ferroelectric with a Zeroâ€Dimensional Perovskiteâ€like Structure. Angewandte Chemie - International Edition, 2016, 55, 11854-11858.	13.8	128
44	Syntheses, crystal structures and properties of two novel lanthanide–carboxylate polymeric complexes. Dalton Transactions RSC, 2002, , 1847-1851.	2.3	126
45	A family of doped lanthanide metal–organic frameworks for wide-range temperature sensing and tunable white light emission. Journal of Materials Chemistry C, 2017, 5, 1981-1989.	5.5	125
46	An Unprecedented Pillarâ€Cage Fluorinated Hybrid Porous Framework with Highly Efficient Acetylene Storage and Separation. Angewandte Chemie - International Edition, 2021, 60, 7547-7552.	13.8	120
47	Stable porphyrin Zr and Hf metal–organic frameworks featuring 2.5 nm cages: high surface areas, SCSC transformations and catalyses. Chemical Science, 2015, 6, 3466-3470.	7.4	118
48	Plastic Transition to Switch Nonlinear Optical Properties Showing the Record High Contrast in a Single-Component Molecular Crystal. Journal of the American Chemical Society, 2015, 137, 15660-15663.	13.7	117
49	Roomâ€Temperature Ferroelectric Material Composed of a Twoâ€Dimensional Metal Halide Double Perovskite for Xâ€ray Detection. Angewandte Chemie - International Edition, 2020, 59, 13879-13884.	13.8	116
50	Polarizationâ€Driven Selfâ€Powered Photodetection in a Singleâ€Phase Biaxial Hybrid Perovskite Ferroelectric. Angewandte Chemie - International Edition, 2019, 58, 14504-14508.	13.8	114
51	Exploiting the Bulk Photovoltaic Effect in a 2D Trilayered Hybrid Ferroelectric for Highly Sensitive Polarized Light Detection. Angewandte Chemie - International Edition, 2020, 59, 3933-3937.	13.8	111
52	Hierarchical metal–organic framework nanoflowers for effective CO <sub>2</sub> transformation driven by visible light. Journal of Materials Chemistry A, 2015, 3, 15764-15768.	10.3	110
53	High-Temperature Antiferroelectric of Lead Iodide Hybrid Perovskites. Journal of the American Chemical Society, 2019, 141, 12470-12474.	13.7	108
54	Electricâ€Field Assisted Inâ€Situ Hydrolysis of Bulk Metal–Organic Frameworks (MOFs) into Ultrathin Metal Oxyhydroxide Nanosheets for Efficient Oxygen Evolution. Angewandte Chemie - International Edition, 2020, 59, 13101-13108.	13.8	108

#	Article	IF	CITATIONS
55	A palladium chelating complex of ionic water-soluble nitrogen-containing ligand: the efficient precatalyst for Suzuki–Miyaura reaction in water. Green Chemistry, 2011, 13, 2100.	9.0	106
56	A non-interpenetrated porous metal–organic framework with high gas-uptake capacity. Chemical Communications, 2011, 47, 9861.	4.1	106
57	Spacer Cation Alloying of a Homoconformational Carboxylate <i>trans</i> Isomer to Boost in-Plane Ferroelectricity in a 2D Hybrid Perovskite. Journal of the American Chemical Society, 2021, 143, 2130-2137.	13.7	106
58	A novel luminescent 3D polymer containing silver chains formed by ligand unsupported Ag–Ag interactions and organic spacers. Dalton Transactions RSC, 2002, , 291.	2.3	99
59	The 3D Channel Framework Based on Indium(III)-btec, and Its Ion-Exchange Properties (btec =) Tj ETQq1 1 0.7843	814 rgBT / 2.0	Oyerlock 10
60	Two Types of 2D Layered Iodoargentates Based on Trimeric [Ag <sub>3</sub> 1 <sub>7</sub> ] Secondary Building Units and Hexameric [Ag <sub>6</sub> 1 <sub>12</sub> ] Ternary Building Units: Syntheses, Crystal Structures, and Efficient Visible Light Responding Photocatalytic Properties. Inorganic Chemistry, 2015, 54, 10593-10603.	4.0	94
61	Trilayered Lead Chloride Perovskite Ferroelectric Affording Self-Powered Visible-Blind Ultraviolet Photodetection with Large Zero-Bias Photocurrent. Journal of the American Chemical Society, 2020, 142, 55-59.	13.7	93
62	An unusual bifunctional Tb-MOF for highly sensitive sensing of Ba <sup>2+</sup> ions and with remarkable selectivities for CO <sub>2</sub> –N <sub>2</sub> and CO <sub>2</sub> –CH <sub>4</sub> . Journal of Materials Chemistry A, 2015, 3, 13526-13532.	10.3	91
63	Cooperation of Three Chromophores Generates the Waterâ€Resistant Nitrate Nonlinear Optical Material Bi <sub>3</sub> TeO <sub>6</sub> OH(NO <sub>3</sub> ) <sub>2</sub> . Angewandte Chemie - International Edition, 2017, 56, 540-544.	13.8	91
64	pH-Responsive chelating N-heterocyclic dicarbene palladium(ii) complexes: recoverable precatalysts for Suzuki–Miyaura reaction in pure water. Green Chemistry, 2011, 13, 2071.	9.0	90
65	Cageâ€Like Porous Materials with Simultaneous High C <sub>2</sub> H <sub>2</sub> Storage and Excellent C <sub>2</sub> H <sub>2</sub> /CO <sub>2</sub> Separation Performance. Angewandte Chemie - International Edition, 2021, 60, 10828-10832.	13.8	90
66	Rational Design and Growth of MOFâ€onâ€MOF Heterostructures. Small, 2021, 17, e2100607.	10.0	90
67	Fabrication of a Robust Lanthanide Metal–Organic Framework as a Multifunctional Material for Fe(III) Detection, CO <sub>2</sub> Capture, and Utilization. Crystal Growth and Design, 2018, 18, 2956-2963.	3.0	89
68	Designing a Deep-UV Nonlinear Optical Fluorooxosilicophosphate. Journal of the American Chemical Society, 2020, 142, 6472-6476.	13.7	89
69	Ferroelastic phase transition and switchable dielectric behavior associated with ordering of molecular motion in a perovskite-like architectured supramolecular cocrystal. Journal of Materials Chemistry C, 2013, 1, 2561.	5.5	88
70	Tailoring of a visible-light-absorbing biaxial ferroelectric towards broadband self-driven photodetection. Nature Communications, 2021, 12, 284.	12.8	86
71	A Prototypical Zeolitic Lanthanideâ~'Organic Framework with Nanotubular Structure. Crystal Growth and Design, 2008, 8, 166-168.	3.0	85
72	Tailor-made porosities of fluorene-based porous organic frameworks for the pre-designable fabrication of palladium nanoparticles with size, location and distribution control. Chemical Science, 2016, 7, 2188-2194.	7.4	84

#	Article	IF	CITATIONS
73	Using cuprophilicity as a multi-responsive chromophore switching color in response to temperature, mechanical force and solvent vapors. Journal of Materials Chemistry C, 2013, 1, 4339.	5.5	83
74	Bulk crystal growth and characterization of imidazolium l-tartrate (IMLT): a novel organic nonlinear optical material with a high laser-induced damage threshold. CrystEngComm, 2013, 15, 2157.	2.6	80
75	A paramagnetic lamellar polymer with a high semiconductivity. Chemical Communications, 2001, , 1020-1021.	4.1	78
76	Self-Assembly of Discrete M <sub>6</sub> L <sub>8</sub> Coordination Cages Based on a Conformationally Flexible Tripodal Phosphoric Triamide Ligand. Inorganic Chemistry, 2012, 51, 4116-4122.	4.0	77
77	Discovery of an Above-Room-Temperature Antiferroelectric in Two-Dimensional Hybrid Perovskite. Journal of the American Chemical Society, 2019, 141, 3812-3816.	13.7	77
78	Formation of an Infinite Three-Dimensional Water Network by the Hierarchic Assembly of Bilayer Water Nanotubes of Octamers. Crystal Growth and Design, 2007, 7, 1385-1387.	3.0	72
79	Heterometallic cluster-based indium–organic frameworks. Chemical Communications, 2014, 50, 15224-15227.	4.1	72
80	A Potential Sn-Based Hybrid Perovskite Ferroelectric Semiconductor. Journal of the American Chemical Society, 2020, 142, 1159-1163.	13.7	72
81	Bandgap Narrowing of Lead-Free Perovskite-Type Hybrids for Visible-Light-Absorbing Ferroelectric Semiconductors. Journal of Physical Chemistry Letters, 2017, 8, 2012-2018.	4.6	71
82	Tailored Engineering of an Unusual (C <sub>4</sub> H <sub>9</sub> NH <sub>3</sub> ) <sub>2</sub> (CH <sub>3</sub> NH <sub>3</sub> ) <sub>2</sub> Twoâ€Dimensional Multilayered Perovskite Ferroelectric for a Highâ€Performance Photodetector. Angewandte Chemie, 2017, 129, 12318-12322.	sub>Pb <si 2.0</si 	ub>3B
83	Precisely Embedding Active Sites into a Mesoporous Zr-Framework through Linker Installation for High-Efficiency Photocatalysis. Journal of the American Chemical Society, 2020, 142, 15020-15026.	13.7	71
84	The Large Secondâ€Harmonic Generation of LiCs <sub>2</sub> PO <sub>4</sub> is caused by the Metalâ€Cationâ€Centered Groups. Angewandte Chemie - International Edition, 2018, 57, 3933-3937.	13.8	70
85	Tuning the Ionicity of Stable Metal–Organic Frameworks through Ionic Linker Installation. Journal of the American Chemical Society, 2019, 141, 3129-3136.	13.7	70
86	In vitro upconverting/downshifting luminescent detection of tumor markers based on Eu <sup>3+</sup> -activated core–shell–shell lanthanide nanoprobes. Chemical Science, 2016, 7, 5013-5019.	7.4	68
87	Self-Assembly of Three CdII- and CuII-Containing Coordination Polymers from 4,4′-Dipyridyl Disulfide. European Journal of Inorganic Chemistry, 2003, 2003, 3623-3632.	2.0	67
88	A combination of multiple chromophores enhances second-harmonic generation in a nonpolar noncentrosymmetric oxide: CdTeMoO6. Journal of Materials Chemistry C, 2013, 1, 2906.	5.5	67
89	Incorporation of In <sub>2</sub> S <sub>3</sub> Nanoparticles into a Metal–Organic Framework for Ultrafast Removal of Hg from Water. Inorganic Chemistry, 2018, 57, 4891-4897.	4.0	67
90	Europium and Terbium Coordination Polymers Assembled from Hexacarboxylate Ligands: Structures and Luminescent Properties. Crystal Growth and Design, 2014, 14, 1010-1017.	3.0	65

#	Article	IF	CITATIONS
91	Flexible Zirconium MOFs as Bromineâ€Nanocontainers for Bromination Reactions under Ambient Conditions. Angewandte Chemie - International Edition, 2017, 56, 14622-14626.	13.8	65
92	Exploring a Polar Twoâ€dimensional Multiâ€layered Hybrid Perovskite of (C <sub>5</sub> H <sub>11</sub> NH <sub>3</sub> ) <sub>2</sub> (CH <sub>3</sub> NH <sub>)Pb<sub for Ultrafastâ€Responding Photodetection. Laser and Photonics Reviews, 2018, 12, 1800060.</sub </sub>	ı>2≪ <b> s</b> ub>l∘	<subb∋7< sub=""></subb∋7<>
93	Syntheses, structures, electrochemistry and magnetic properties of chain-like dicyanamide manganese(iii) and iron(iii) complexes with salen ligand. New Journal of Chemistry, 2002, 26, 1397-1401.	2.8	63
94	Two Novel Inorganic-Organic Hybrid Frameworks Based on InIII-BTC and InIII-BTEC. European Journal of Inorganic Chemistry, 2005, 2005, 77-81.	2.0	63
95	Fabricating a super stable luminescent chemosensor with multi-stimuli-response to metal ions and small organic molecules through turn-on and turn-off effects. Journal of Materials Chemistry C, 2017, 5, 4511-4519.	5.5	63
96	Mixed-Lanthanide Metal–Organic Frameworks with Tunable Color and White Light Emission. Crystal Growth and Design, 2017, 17, 940-944.	3.0	62
97	Cd(II)-sulfonyldibenzoilate coordination polymers based on mono-, bi-, tri- and tetranuclear cores as nodes. CrystEngComm, 2008, 10, 905.	2.6	61
98	Rapid and discriminative detection of nitro aromatic compounds with high sensitivity using two zinc MOFs synthesized through a temperature-modulated method. Journal of Materials Chemistry A, 2015, 3, 22369-22376.	10.3	61
99	From Nonluminescent to Blueâ€Emitting Cs <sub>4</sub> PbBr <sub>6</sub> Nanocrystals: Tailoring the Insulator Bandgap of 0D Perovskite through Sn Cation Doping. Advanced Materials, 2019, 31, e1900606.	21.0	61
100	An Exceptional Peroxide Birefringent Material Resulting from d–π Interactions. Angewandte Chemie - International Edition, 2020, 59, 9414-9417.	13.8	60
101	Halide Double Perovskite Ferroelectrics. Angewandte Chemie - International Edition, 2020, 59, 9305-9308.	13.8	60
102	From discrete octahedral nanocages to 1D coordination polymer: Coordination-driven a single-crystal-to-single-crystal transformation via anion exchange. Chemical Communications, 2011, 47, 2327-2329.	4.1	59
103	Visualizing the Dynamics of Temperature―and Solventâ€Responsive Soft Crystals. Angewandte Chemie - International Edition, 2016, 55, 7478-7482.	13.8	59
104	Superior thermoelasticity and shape-memory nanopores in a porous supramolecular organic framework. Nature Communications, 2016, 7, 11564.	12.8	58
105	An Anionic Uranium-Based Metal–Organic Framework with Ultralarge Nanocages for Selective Dye Adsorption. Crystal Growth and Design, 2018, 18, 576-580.	3.0	58
106	Ultrasensitive polarized-light photodetectors based on 2D hybrid perovskite ferroelectric crystals with a low detection limit. Science Bulletin, 2021, 66, 158-163.	9.0	58
107	Anodic formation of nanoporous and nanotubular metal oxides. Journal of Materials Chemistry, 2012, 22, 535-544.	6.7	57
108	Interconvertible vanadium-seamed hexameric pyrogallol[4]arene nanocapsules. Nature Communications, 2018, 9, 4941.	12.8	57

#	Article	IF	CITATIONS
109	Coexistence of cages and one-dimensional channels in a porous MOF with high H2 and CH4 uptakes. Chemical Communications, 2014, 50, 2834.	4.1	55
110	Secondâ€Order Nonlinear Optical Switch of a New Hydrogenâ€Bonded Supramolecular Crystal with a High Laserâ€Induced Damage Threshold. Advanced Optical Materials, 2014, 2, 1199-1205.	7.3	55
111	Strong Nonlinear-Optical Response in the Pyrophosphate CsLiCdP <sub>2</sub> O <sub>7</sub> with a Short Cutoff Edge. Inorganic Chemistry, 2016, 55, 11626-11629.	4.0	55
112	A semi-conductive organic–inorganic hybrid emits pure white light with an ultrahigh color rendering index. Journal of Materials Chemistry C, 2017, 5, 4731-4735.	5.5	55
113	Biodegradable Inorganic Upconversion Nanocrystals for <i>In Vivo</i> Applications. ACS Nano, 2020, 14, 16672-16680.	14.6	55
114	Two New Zeolite-Like Supramolecular Copper Complexes. European Journal of Inorganic Chemistry, 2003, 2003, 94-98.	2.0	54
115	Stepwise Construction of Extra-Large Heterometallic Calixarene-Based Cages. Inorganic Chemistry, 2015, 54, 3183-3188.	4.0	53
116	Design of metal-organic NLO materials: complexes derived from pyridine-3,4-dicarboxylate. New Journal of Chemistry, 2004, 28, 1590.	2.8	52
117	Self-Assembly Syntheses, Structural Characterization, and Luminescent Properties of Lanthanide Coordination Polymers Constructed by Three Triazole-Carboxylate Ligands. Crystal Growth and Design, 2016, 16, 2266-2276.	3.0	51
118	Giant and Broadband Multiphoton Absorption Nonlinearities of a 2D Organometallic Perovskite Ferroelectric. Advanced Materials, 2020, 32, e2002972.	21.0	51
119	Constructing Crystalline Heterometallic Indium–Organic Frameworks by the Bifunctional Method. Crystal Growth and Design, 2015, 15, 1440-1445.	3.0	50
120	Self-Assembly of a One-Dimensional Silver Complex Containing Two Kinds of Helical Chains. European Journal of Inorganic Chemistry, 2003, 2003, 38-41.	2.0	49
121	High-Performance Switching of Bulk Quadratic Nonlinear Optical Properties with Large Contrast in Polymer Films Based on Organic Hydrogen-Bonded Ferroelectrics. Chemistry of Materials, 2015, 27, 4493-4498.	6.7	49
122	Controlled Orthogonal Selfâ€Assembly of Heterometalâ€Decorated Coordination Cages. Chemistry - A European Journal, 2016, 22, 17345-17350.	3.3	49
123	Syntheses and Crystal Structures of Five Cadmium(II) Complexes Derived from 4-Aminobenzoic Acid. European Journal of Inorganic Chemistry, 2002, 2002, 2904-2912.	2.0	47
124	New Types of Homochiral Helical Coordination Polymers Constructed byexo-Bidentate Binaphthol Derivatives. European Journal of Inorganic Chemistry, 2004, 2004, 1595-1599.	2.0	46
125	A Nonlinear Optical Switchable Sulfate of Ultrawide Bandgap. CCS Chemistry, 2021, 3, 2298-2306.	7.8	46
126	Synthesis and Crystal Structures of the First Two Novel Dicarboxylate Organotin Polymers Constructed from Dimeric Tetraorganodistannoxane Units. European Journal of Inorganic Chemistry, 2002, 2002, 2082-2085.	2.0	45

#	Article	IF	CITATIONS
127	Metal-Directed Self-Assembly: Two New Metal-Binicotinate Grid Polymeric Networks and Their Fluorescence Emission Tuned by Ligand Configuration. European Journal of Inorganic Chemistry, 2004, 2004, 2695-2700.	2.0	45
128	Engineering of Acentric Stilbazolium Salts with Large Second-Order Optical Nonlinearity and Enhanced Environmental Stability. Crystal Growth and Design, 2012, 12, 6181-6187.	3.0	44
129	Magnetic Properties of 3D Heptanuclear Lanthanide Frameworks Supported by Mixed Ligands. Inorganic Chemistry, 2015, 54, 6081-6083.	4.0	44
130	A general strategy for tailoring upconversion luminescence in lanthanide-doped inorganic nanocrystals through local structure engineering. Nanoscale, 2018, 10, 9353-9359.	5.6	44
131	A Multiaxial Layered Halide Double Perovskite Ferroelectric with Multiple Ferroic Orders. Chemistry of Materials, 2020, 32, 8965-8970.	6.7	44
132	Mono- and Bilayered Lead(II)-bpno Polymers with Unusual Low Energy Emission Properties (bpno =) Tj ETQq0 0	0 rgBT /Ov	erlock 10 Tf 5
133	Luminescent sensing profiles based on anion-responsive lanthanide( <scp>iii</scp> ) quinolinecarboxylate materials: solid-state structures, photophysical properties, and anionic species recognition. Journal of Materials Chemistry C, 2015, 3, 2003-2015.	5.5	43
134	Structural variability, unusual thermochromic luminescence and nitrobenzene sensing properties of five Zn( <scp>ii</scp> ) coordination polymers assembled from a terphenyl-hexacarboxylate ligand. CrystEngComm, 2015, 17, 3829-3837.	2.6	43
135	Manipulating energy transfer in lanthanide-doped single nanoparticles for highly enhanced upconverting luminescence. Chemical Science, 2017, 8, 5050-5056.	7.4	43
136	Nonpolar Na <sub>10</sub> Cd(NO <sub>3</sub> ) <sub>4</sub> (SO <sub>3</sub> S) <sub>4</sub> Exhibits a Large Second-Harmonic Generation. CCS Chemistry, 2022, 4, 526-531.	7.8	43
137	A seed-mediated approach to the general and mild synthesis of non-noble metal nanoparticles stabilized by a metal–organic framework for highly efficient catalysis. Materials Horizons, 2015, 2, 606-612.	12.2	42
138	Highly Sensitive and Ultrafast Responding Array Photodetector Based on a Newly Tailored 2D Lead Iodide Perovskite Crystal. Advanced Optical Materials, 2019, 7, 1900308.	7.3	42
139	Unconventional inorganic precursors determine the growth of metal-organic frameworks. Coordination Chemistry Reviews, 2021, 434, 213804.	18.8	42
140	Centimeter-Sized Single Crystal of a One-Dimensional Lead-Free Mixed-Cation Perovskite Ferroelectric for Highly Polarization Sensitive Photodetection. Journal of the American Chemical Society, 2021, 143, 16758-16767.	13.7	42
141	A nucleobase–inorganic hybrid polymer consisting of copper bis(phosphopentamolybdate) and cytosine. Dalton Transactions RSC, 2002, , 289-290.	2.3	41
142	Cuboctahedron-based indium–organic frameworks for gas sorption and selective cation exchange. Chemical Communications, 2016, 52, 7978-7981.	4.1	41
143	Induction of Chirality in a Metal–Organic Framework Built from Achiral Precursors. Angewandte Chemie - International Edition, 2021, 60, 3087-3094.	13.8	41
144	Self-Assembly of Five Cadmium(II) Coordination Polymers from 4,4′-Diaminodiphenylmethane. European Journal of Inorganic Chemistry, 2003, 2003, 1778-1784.	2.0	40

#	Article	IF	CITATIONS
145	pH modulated assembly in the mixed-ligand system Cd(ii)–dpstc–phen: structural diversity and luminescent properties. CrystEngComm, 2013, 15, 3992.	2.6	40
146	A controllable and dynamic assembly system based on discrete metallocages. Chemical Science, 2014, 5, 483-488.	7.4	40
147	Solvent and temperature influence structural variation from nonporous 2D → 3D parallel polycatenation to 3D microporous metal–organic framework. CrystEngComm, 2011, 13, 3971.	2.6	39
148	ZnTeMoO6: a strong second-harmonic generation material originating from three types of asymmetric building units. RSC Advances, 2013, 3, 14000.	3.6	39
149	Constructing π-Stacked Supramolecular Cage Based Hierarchical Self-Assemblies via π···π Stacking and Hydrogen Bonding. Journal of the American Chemical Society, 2021, 143, 10920-10929.	13.7	39
150	Chiral Supramolecular Assemblies Derived from the Insertion of a Segmental Ligand into a Copper-Tyrosine Framework. European Journal of Inorganic Chemistry, 2002, 2002, 2553-2556.	2.0	38
151	Self-Assembly of Novel Silver Polymers Based on Flexible Sulfonate Ligands. European Journal of Inorganic Chemistry, 2004, 2004, 2144-2150.	2.0	38
152	Syntheses, Structures, and Characterization of Two Manganese(II)-Aminobenzoic Complexes. European Journal of Inorganic Chemistry, 2006, 2006, 1649-1656.	2.0	38
153	Thermally stable helical chain and octanuclear Ag(I) coordination networks with yellow luminescence. CrystEngComm, 2009, 11, 2529.	2.6	38
154	A Photoferroelectric Perovskiteâ€Type Organometallic Halide with Exceptional Anisotropy of Bulk Photovoltaic Effects. Angewandte Chemie, 2016, 128, 6655-6660.	2.0	38
155	A monomeric bowl-like pyrogallol[4]arene Ti <sub>12</sub> coordination complex. Chemical Communications, 2017, 53, 9598-9601.	4.1	38
156	3D lanthanide–transition-metal–organic frameworks constructed from tetranuclear {Ln4} SBUs and Cu centres with fsc net. CrystEngComm, 2011, 13, 3998.	2.6	37
157	Cation-Induced Strategy toward an Hourglass-Shaped Cu <sub>6</sub> I <sub>7</sub> <sup>–</sup> Cluster and Its Color-Tunable Luminescence. Chemistry of Materials, 2017, 29, 8093-8099.	6.7	37
158	Soft Perovskite-Type Antiferroelectric with Giant Electrocaloric Strength near Room Temperature. Journal of the American Chemical Society, 2020, 142, 20744-20751.	13.7	37
159	Cation-doping matters in caesium lead halide perovskite nanocrystals: from physicochemical fundamentals to optoelectronic applications. Nanoscale, 2020, 12, 12228-12248.	5.6	37
160	A Deepâ€UV Nonlinear Optical Borosulfate with Incommensurate Modulations. Angewandte Chemie - International Edition, 2021, 60, 11457-11463.	13.8	37
161	Syntheses and structural characterization of silver(I) complexes with versatile heterocyclic sulfur and nitrogen donor ligands. Polyhedron, 2001, 20, 2619-2625.	2.2	36
162	A Series of d <sup>10</sup> Metal Clusters Constructed by 2,6-Bis[3-(pyrazin-2-yl)-1,2,4-triazolyl]pyridine: Crystal Structures and Unusual Luminescences. Crystal Growth and Design, 2014, 14, 5011-5018.	3.0	36

#	Article	IF	CITATIONS
163	The dynamic response of a flexible indium based metal–organic framework to gas sorption. Chemical Communications, 2016, 52, 2277-2280.	4.1	36
164	Dynamic Formation of Coordination Polymers versus Tetragonal Prisms and Unexpected Magnetic Superexchange Coupling Mediated by Encapsulated Anions in the Cobalt(II) 1,3-Bis(pyrid-4-ylthio)propan-2-one Series. Inorganic Chemistry, 2005, 44, 9175-9184.	4.0	35
165	A solid AND logic stimuli-responsive material with bright nondestructive performance designed by sensitive cuprophilicity. Chemical Communications, 2013, 49, 10227.	4.1	35
166	Intrinsic Strong Linear Dichroism of Multilayered 2D Hybrid Perovskite Crystals toward Highly Polarizedâ€Sensitive Photodetection. Advanced Optical Materials, 2019, 7, 1901049.	7.3	35
167	Solutionâ€Grown Largeâ€5ized Singleâ€Crystalline 2D/3D Perovskite Heterostructure for Selfâ€Powered Photodetection. Advanced Optical Materials, 2020, 8, 2000311.	7.3	35
168	[(N-AEPz)ZnCl <sub>4</sub> ]Cl: A "Green―Metal Halide Showing Highly Efficient Bluish-White-Light Emission. Inorganic Chemistry, 2020, 59, 3527-3531.	4.0	35
169	An Unprecedented Antimony(III) Borate with Strong Linear and Nonlinear Optical Responses. Angewandte Chemie, 2020, 132, 7867-7870.	2.0	35
170	Synthesis and Characterization of a 3D H-Bonded Supramolecular Complex with Chiral Channels Encapsulating 1D Left-Handed Helical Water Chains. European Journal of Inorganic Chemistry, 2005, 2005, 3214-3216.	2.0	34
171	Sorption behaviour in a unique 3,12-connected zinc–organic framework with 2.4 nm cages. Journal of Materials Chemistry A, 2013, 1, 10631.	10.3	34
172	Structural Diversity Modulated by the Ratios of a Ternary Solvent Mixture: Syntheses, Structures, and Luminescent Properties of Five Zinc(II) Metal–Organic Frameworks. Crystal Growth and Design, 2015, 15, 1481-1491.	3.0	34
173	A photoluminescent indium–organic framework with discrete cages and one-dimensional channels for gas adsorption. Chemical Communications, 2016, 52, 9032-9035.	4.1	34
174	An indium–organic framework for the efficient storage of light hydrocarbons and selective removal of organic dyes. Dalton Transactions, 2019, 48, 5527-5533.	3.3	34
175	Synthesis and characterization of two copper cyanide complexes with hexagonal Cu6 units. Dalton Transactions RSC, 2000, , 1685-1686.	2.3	33
176	Synthesis, growth and characterization of a third-order nonlinear optical crystal based on the borate ester with sodium supporting its structural framework. New Journal of Chemistry, 2011, 35, 2804.	2.8	33
177	Anion-driven self-assembly: from discrete cages to infinite polycatenanes step by step. Chemical Communications, 2013, 49, 719-721.	4.1	32
178	A Flexible Twoâ€Fold Interpenetrated Indium MOF Exhibiting Dynamic Response to Gas Adsorption and Highâ€Sensitivity Detection of Nitroaromatic Explosives. Chemistry - an Asian Journal, 2019, 14, 3597-3602.	3.3	32
179	Constructing Allâ€Inorganic Perovskite/Fluoride Nanocomposites for Efficient and Ultraâ€Stable Perovskite Solar Cells. Advanced Functional Materials, 2021, 31, 2106386.	14.9	32
180	Achieving gas pressure-dependent luminescence from an AlEgen-based metal-organic framework. Nature Communications, 2022, 13, 2142.	12.8	32

#	Article	IF	CITATIONS
181	Two dual-emissive Zn(ii) coordination polymers with tunable photoluminescence properties. CrystEngComm, 2012, 14, 6394.	2.6	31
182	Anion-controlled conformational variation: Structural modulation and anion exchange of Ag( <scp>i</scp> ) coordination networks. CrystEngComm, 2012, 14, 1693-1700.	2.6	31
183	A water-stable 3D Eu-MOF based on a metallacyclodimeric secondary building unit for sensitive fluorescent detection of acetone molecules. CrystEngComm, 2019, 21, 321-328.	2.6	31
184	Roomâ€Temperature Ferroelectric Material Composed of a Twoâ€Dimensional Metal Halide Double Perovskite for Xâ€ray Detection. Angewandte Chemie, 2020, 132, 13983-13988.	2.0	31
185	Minuteâ€Scale Rapid Crystallization of a Highly Dichroic 2D Hybrid Perovskite Crystal toward Efficient Polarizationâ€Sensitive Photodetector. Advanced Optical Materials, 2020, 8, 2000149.	7.3	31
186	Combinatorial Selfâ€Assembly of Coordination Cages with Systematically Fineâ€Tuned Cavities for Efficient Coâ€Encapsulation and Catalysis. Angewandte Chemie - International Edition, 2022, 61, .	13.8	31
187	Auxiliary ligand-directed and counter anion-templated effects on coordination networks based on semirigid 2-aminodiacetic terephthalic acid ligand. CrystEngComm, 2013, 15, 911-921.	2.6	30
188	Unusual Long-Range Ordering Incommensurate Structural Modulations in an Organic Molecular Ferroelectric. Journal of the American Chemical Society, 2017, 139, 15900-15906.	13.7	30
189	Solvent-Assisted, Thermally Triggered Structural Transformation in Flexible Mesoporous Metal–Organic Frameworks. Chemistry of Materials, 2019, 31, 8787-8793.	6.7	30
190	Increase in pore size and gas uptake capacity in indium-organic framework materials. Journal of Materials Chemistry A, 2013, 1, 9075.	10.3	29
191	Bridging different Co <sub>4</sub> –calix[4]arene building blocks into grids, cages and 2D polymers with chiral camphoric acid. CrystEngComm, 2015, 17, 1750-1753.	2.6	29
192	Highly Oriented Thin Films of 2D Ruddlesdenâ€Popper Hybrid Perovskite toward Superfast Response Photodetectors. Small, 2019, 15, e1901194.	10.0	29
193	Rational design of high-quality 2D/3D perovskite heterostructure crystals for record-performance polarization-sensitive photodetection. National Science Review, 2021, 8, nwab044.	9.5	29
194	Thermochromism to tune the optical bandgap of a lead-free perovskite-type hybrid semiconductor for efficiently enhancing photocurrent generation. Journal of Materials Chemistry C, 2017, 5, 9967-9971.	5.5	28
195	Polarizationâ€Driven Selfâ€Powered Photodetection in a Singleâ€Phase Biaxial Hybrid Perovskite Ferroelectric. Angewandte Chemie, 2019, 131, 14646-14650.	2.0	28
196	Highly Elastic Anti-fatigue and Anti-freezing Conductive Double Network Hydrogel for Human Body Sensors. Industrial & Engineering Chemistry Research, 2021, 60, 6162-6172.	3.7	28
197	Syntheses and Characterizations of Metal-Organic Frameworks with Unusual Topologies Derived from Flexible Dipyridyl Ligands. European Journal of Inorganic Chemistry, 2004, 2004, 3751.	2.0	27
198	An Ultrastable π–π Stacked Porous Organic Molecular Framework as a Crystalline Sponge for Rapid Molecular Structure Determination. CCS Chemistry, 2022, 4, 1315-1325.	7.8	27

#	Article	IF	CITATIONS
199	Whiteâ€Light Emission and Circularly Polarized Luminescence from a Chiral Copper(I) Coordination Polymer through Symmetryâ€Breaking Crystallization. Angewandte Chemie - International Edition, 2022, 61, .	13.8	27
200	Tailoring the Distinctive Chiralâ€Polar Perovskites with Alternating Cations in the Interlayer Space for Selfâ€Đriven Circularly Polarized Light Detection. Advanced Optical Materials, 2022, 10, .	7.3	27
201	Title is missing!. Journal of Cluster Science, 2002, 13, 33-41.	3.3	26
202	The 3D porous metal–organic frameworks based on bis(pyrazinyl)–trizole: structures, photoluminescence and gas adsorption properties. CrystEngComm, 2013, 15, 5673.	2.6	26
203	Alloying <i>n</i> â€Butylamine into CsPbBr <sub>3</sub> To Give a Twoâ€Dimensional Bilayered Perovskite Ferroelectric Material. Angewandte Chemie, 2018, 130, 8272-8275.	2.0	26
204	A Molecular Ferroelectric Showing Roomâ€Temperature Recordâ€Fast Switching of Spontaneous Polarization. Angewandte Chemie - International Edition, 2018, 57, 9833-9837.	13.8	26
205	A Robust Multifunctional Eu <sub>6</sub> -Cluster Based Framework for Gas Separation and Recognition of Small Molecules and Heavy Metal Ions. Crystal Growth and Design, 2019, 19, 6381-6387.	3.0	26
206	Incorporating Three Chiral Channels into an In-MOF for Excellent Gas Absorption and Preliminary Cu <sup>2+</sup> Ion Detection. Crystal Growth and Design, 2019, 19, 3860-3868.	3.0	26
207	Oxidation-State and Coordination-Site Specificity Influencing Dimensional Extension and Properties of Two Iron Complexes with Similar Helical Chains. European Journal of Inorganic Chemistry, 2004, 2004, 4457-4462.	2.0	25
208	Stabilizing the Extrinsic Porosity in Metal–Organic Cages-Based Supramolecular Framework by In Situ Catalytic Polymerization. CCS Chemistry, 2021, 3, 1382-1390.	7.8	25
209	The First Two Novel Metallomacrocycles Constructed from Cubane-Like Cu4l4 Cluster Units and Ditopic Diamines. European Journal of Inorganic Chemistry, 2002, 2002, 3097-3100.	2.0	24
210	Indium(iii)-2,5-pyridine dicarboxylate complexes with mononuclear, 1D chain, 2D layer and 3D chiral frameworks. CrystEngComm, 2009, 11, 918.	2.6	24
211	Iodide-Centered Cuprous Octatomic Ring: A Luminescent Molecular Thermometer Exhibiting Dual-Emission Character. Crystal Growth and Design, 2018, 18, 22-26.	3.0	24
212	Azobenzene Decorated NbO-Type Metal–Organic Framework for High-Capacity Storage of Energy Gases. Inorganic Chemistry, 2019, 58, 11983-11987.	4.0	24
213	Construction of a Stable Lanthanide Metal-Organic Framework as a Luminescent Probe for Rapid Naked-Eye Recognition of Fe3+ and Acetone. Molecules, 2021, 26, 1695.	3.8	24
214	Highly Efficient White-Light Emission Induced by Carboxylic Acid Dimers in a Layered Hybrid Perovskite. CCS Chemistry, 2022, 4, 2491-2497.	7.8	24
215	Effect of Conformation and Combination of 1,3-Bis(4-pyridylthio)propan-2-one upon Coordination Architectures: Syntheses, Characterizations and Properties. European Journal of Inorganic Chemistry, 2005, 2005, 1303-1311.	2.0	23
216	High performance self-powered photodetection with a low detection limit based on a two-dimensional organometallic perovskite ferroelectric. Journal of Materials Chemistry C, 2021, 9, 881-887.	5.5	23

#	Article	IF	CITATIONS
217	Chiral Leadâ€Free Hybrid Perovskites for Selfâ€Powered Circularly Polarized Light Detection. Angewandte Chemie, 2021, 133, 8496-8499.	2.0	23
218	A Novel Two-Dimensional Layer Structure Built from a Tetracobalt(II)-p-sulfonatothiacalix[4]arene Cluster Unit. European Journal of Inorganic Chemistry, 2005, 2005, 1182-1187.	2.0	22
219	Five novel Zn( <scp>ii</scp> )/Cd( <scp>ii</scp> ) coordination polymers based on bis(pyrazinyl)-triazole and varied polycarboxylates: syntheses, topologies and photoluminescence. CrystEngComm, 2014, 16, 11078-11087.	2.6	22
220	Engineering Oxygen Vacancies in Mesocrystalline CuO Nanosheets for Water Oxidation. ACS Applied Nano Materials, 2021, 4, 6135-6144.	5.0	22
221	Heterooctanuclear Cluster Complex Formation with Phosphine Participation:Â Synthesis, Structure, and Magnetic Properties of Co6Ru2(mp)10(PBun3)6(H2mp = 2-Mercaptophenol, PBun3=) Tj ETQq1 1 0.784314	rg₿₫ /Ove	erlæak 10 Tf 5
222	From 3D interpenetrated polythreading to 3D non-interpenetrated polythreading: SBU modulation in a dual-ligand system. CrystEngComm, 2014, 16, 1249-1252.	2.6	21
223	Diverse architectures and luminescence properties of two novel copper( <scp>i</scp> ) coordination polymers assembled from 2,6-bis[3-(pyrid-4-yl)-1,2,4-triazolyl]pyridine ligands. CrystEngComm, 2015, 17, 1541-1548.	2.6	21
224	Introduction of Flexibility into a Metal–Organic Framework to Promote Hg(II) Capture through Adaptive Deformation. Inorganic Chemistry, 2020, 59, 18264-18275.	4.0	21
225	Sustained Antitumor Immunity Based on Persistent Luminescence Nanoparticles for Cancer Immunotherapy. Advanced Functional Materials, 2021, 31, 2106884.	14.9	21
226	Metal-Directed Stereoselective Syntheses of Homochiral Complexes ofexo-Bidentate Binaphthol Derivatives. European Journal of Inorganic Chemistry, 2005, 2005, 751-758.	2.0	20
227	Exploring a Leadâ€free Semiconducting Hybrid Ferroelectric with a Zeroâ€Dimensional Perovskiteâ€like Structure. Angewandte Chemie, 2016, 128, 12033-12037.	2.0	20
228	Bistable N–Hâ√N hydrogen bonds for reversibly modulating the dynamic motion in an organic co-crystal. Physical Chemistry Chemical Physics, 2016, 18, 10868-10872.	2.8	20
229	A reduced-dimensional polar hybrid perovskite for self-powered broad-spectrum photodetection. Chemical Science, 2021, 12, 3050-3054.	7.4	20
230	A Noncovalent Ï€â€Stacked Porous Organic Molecular Framework for Selective Separation of Aromatics and Cyclic Aliphatics. Angewandte Chemie - International Edition, 2022, 61, .	13.8	20
231	Temperature-controlled reduction of Cu(ii) and structural transformation on the assembly of coordination network. CrystEngComm, 2012, 14, 4181.	2.6	19
232	A Porous Framework as a Variable Chemosensor: From the Response of a Specific Carcinogenic Alkylâ€Aromatic to Selective Detection of Explosive Nitroaromatics. Chemistry - A European Journal, 2018, 24, 11033-11041.	3.3	19
233	A robust cage-based framework for the highly selective purification of natural gas. Chemical Communications, 2019, 55, 10257-10260.	4.1	19
234	Constructing multi-cluster copper( <scp>i</scp> ) halides using conformationally flexible ligands. Chemical Communications, 2020, 56, 7233-7236.	4.1	19

#	Article	IF	CITATIONS
235	Key Factors Controlling the Large Second Harmonic Generation in Nonlinear Optical Materials. ACS Applied Materials & Interfaces, 2020, 12, 9434-9439.	8.0	19
236	Exploring a Fatigueâ€Free Layered Hybrid Perovskite Ferroelectric for Photovoltaic Nonâ€Volatile Memories. Angewandte Chemie - International Edition, 2021, 60, 10598-10602.	13.8	19
237	Coordination-Driven Face-Directed Self-Assembly of a M <sub>9</sub> L <sub>6</sub> Hexahedral Nanocage from Octahedral Ni(II) Ions and Asymmetric Hydrazone Ligands. Crystal Growth and Design, 2009, 9, 28-31.	3.0	18
238	Controllable Coordination Selfâ€Assembly Based on Flexible Tripodal Ligands: From Finite Metallocages to Infinite Polycatenanes Step by Step. Chemical Record, 2015, 15, 711-727.	5.8	18
239	Crystal structure, morphology and sorption behaviour of porous indium-tetracarboxylate framework materials. CrystEngComm, 2015, 17, 8512-8518.	2.6	18
240	Controllable Reassembly of a Dynamic Metallocage: From Thermodynamic Control to Kinetic Control. Chemistry - A European Journal, 2017, 23, 456-461.	3.3	18
241	Tunable dual-emission luminescence from Cu( <scp>i</scp> )-cluster-based MOFs for multi-stimuli responsive materials. Journal of Materials Chemistry C, 2021, 9, 2890-2897.	5.5	18
242	2D van der Waals Layered [C(NH <sub>2</sub> ) <sub>3</sub> ] <sub>2</sub> SO <sub>3</sub> S Exhibits Desirable UV Nonlinear-Optical Trade-Off. Inorganic Chemistry, 2021, 60, 14544-14549.	4.0	18
243	Syntheses and Crystal Structures of Two Thiolato-Organophosphino Cobalt(II) Complexes, (Et4N)[Co(SC6H5)3(PPh3)] and [Co(S-m-C6H4CH3)2(Ph2PCH2CH2P(Ph)CH2CH2PPh2)]. Journal of Coordination Chemistry, 1992, 25, 183-191.	2.2	17
244	Syntheses, crystal structures and non-linear optical responses of two new heteroselenometallic cluster compounds containing dithiocarbamate ligands. Dalton Transactions RSC, 2000, , 605-610.	2.3	17
245	A novel coordination polymer containing puckered rhombus grids. Dalton Transactions RSC, 2002, , 1354-1357.	2.3	17
246	Lanthanide-Doped KGd <sub>2</sub> F <sub>7</sub> Nanocrystals: Controlled Synthesis, Optical Properties, and Spectroscopic Identification of the Optimum Core/Shell Architecture for Highly Enhanced Upconverting Luminescence. Crystal Growth and Design, 2019, 19, 2340-2349.	3.0	17
247	Halide Double Perovskite Ferroelectrics. Angewandte Chemie, 2020, 132, 9391-9394.	2.0	17
248	Structure and photoluminescent properties of lanthanide coordination polymers based on two isomers of iminodiacetic acid substituted isophthalate and terephthalate ligands. CrystEngComm, 2012, 14, 6055.	2.6	16
249	SO <sub>4</sub> <sup>2â^'</sup> anion directed hexagonal-prismatic cages via cooperative C–Hâ<⁻O hydrogen bonds. Chemical Science, 2014, 5, 4163-4166.	7.4	16
250	3D metal-organic frameworks based on lanthanide-seamed dimeric pyrogallol[4]arene nanocapsules. Science China Chemistry, 2018, 61, 664-669.	8.2	16
251	Exploiting the Bulk Photovoltaic Effect in a 2D Trilayered Hybrid Ferroelectric for Highly Sensitive Polarized Light Detection. Angewandte Chemie, 2020, 132, 3961-3965.	2.0	16
252	Acid–Base-Resistant Metal–Organic Framework for Size-Selective Carbon Dioxide Capture. Inorganic Chemistry, 2020, 59, 13542-13550.	4.0	16

#	Article	IF	CITATIONS
253	Electricâ€Field Assisted Inâ€Situ Hydrolysis of Bulk Metal–Organic Frameworks (MOFs) into Ultrathin Metal Oxyhydroxide Nanosheets for Efficient Oxygen Evolution. Angewandte Chemie, 2020, 132, 13201-13208.	2.0	16
254	Peasecod‣ike Hollow Upconversion Nanocrystals with Excellent Optical Thermometric Performance. Advanced Science, 2020, 7, 2000731.	11.2	16
255	Multilayered 2D Cesiumâ€Based Hybrid Perovskite with Strong Polarization Sensitivity: Dimensional Reduction of CsPbBr <sub>3</sub> . Chemistry - A European Journal, 2020, 26, 3494-3498.	3.3	16
256	Functionalized Metalâ€Organic Frameworks for Hg(II) and Cd(II) Capture: Progresses and Challenges. Chemical Record, 2021, 21, 1455-1472.	5.8	16
257	Nickel-Organic Coordination Layers with Different Directional Cavities. European Journal of Inorganic Chemistry, 2006, 2006, 4852-4856.	2.0	15
258	Double-walled tubular metal–organic frameworks constructed from bi-strand helices. CrystEngComm, 2009, 11, 1831.	2.6	15
259	Topological variability of Zn(ii) and Co(ii) 3D coordination polymers obtained through solvothermal in situ disulfide cleavage. CrystEngComm, 2011, 13, 6323.	2.6	15
260	Conformation driven in situ interlock: from discrete metallocycles to infinite polycatenanes. Chemical Communications, 2015, 51, 13706-13709.	4.1	15
261	Self-assembly of two high-nuclearity manganese calixarene-phosphonate clusters: diamond-like Mn <sub>16</sub> and drum-like Mn <sub>14</sub> . RSC Advances, 2015, 5, 33579-33585.	3.6	15
262	Dependence of the Second-Harmonic Generation Response on the Cell Volume to Band-Gap Ratio. Inorganic Chemistry, 2019, 58, 9572-9575.	4.0	15
263	Tin-Doped Near-Infrared Persistent Luminescence Nanoparticles with Considerable Improvement of Biological Window Activation for Deep Tumor Photodynamic Therapy. ACS Applied Bio Materials, 2020, 3, 5995-6004.	4.6	15
264	Induction of Chirality in a Metal–Organic Framework Built from Achiral Precursors. Angewandte Chemie, 2021, 133, 3124-3131.	2.0	15
265	Condensation of SCH2CH2S2- During the Formation of a Nickel(II) Complex Containing Mixed Ligands. Synthesis and Crystal Structure of Ni(PPh3)(tpdt). Journal of Coordination Chemistry, 1992, 25, 165-169.	2.2	14
266	A new access to palladium–phosphine chemistry. Formation of polynuclear palladium compounds via the oxidation of ligands in simple palladium(II) complexes. Dalton Transactions RSC, 2000, , 1527-1532.	2.3	14
267	A novel trinuclear cobalt complex comprising moieties derived from single and double Cââ,¬â€œS bond cleavage of diethyldithiocarbamate. Dalton Transactions RSC, 2001, , 2961-2962.	2.3	14
268	Second harmonic generation responses of KH <sub>2</sub> PO <sub>4</sub> : importance of K and breaking down of Kleinman symmetry. RSC Advances, 2020, 10, 26479-26485.	3.6	14
269	Metal–organic tube or layered assembly: reversible sheet-to-tube transformation and adaptive recognition. Chemical Science, 2020, 11, 9818-9826.	7.4	14
270	An Exceptional Peroxide Birefringent Material Resulting from d–π Interactions. Angewandte Chemie, 2020, 132, 9500-9503.	2.0	14

#	Article	IF	CITATIONS
271	An ultra-stable microporous supramolecular framework with highly selective adsorption and separation of water over ethanol. Nano Research, 2021, 14, 2584-2588.	10.4	14
272	Unprecedented Self-Powered Visible–Infrared Dual-Modal Photodetection Induced by a Bulk Photovoltaic Effect in a Polar Perovskite. ACS Applied Materials & Interfaces, 2022, 14, 5608-5614.	8.0	14
273	Flexible Zirconium MOFs as Bromineâ€Nanocontainers for Bromination Reactions under Ambient Conditions. Angewandte Chemie, 2017, 129, 14814-14818.	2.0	13
274	A Molecular Ferroelectric Showing Roomâ€Temperature Recordâ€Fast Switching of Spontaneous Polarization. Angewandte Chemie, 2018, 130, 9981-9985.	2.0	13
275	Chiral induction in a <b>pcu</b> -derived network from achiral precursors. Chemical Communications, 2019, 55, 4611-4614.	4.1	13
276	Sorption comparison of two indium–organic framework isomers with syn–anti configurations. CrystEngComm, 2014, 16, 7434.	2.6	12
277	Syntheses, structures, luminescence and magnetic properties of three high-nuclearity neodymium compounds based on mixed sulfonylcalix[4]arene-phosphonate ligands. CrystEngComm, 2016, 18, 4921-4928.	2.6	12
278	Cooperation of Three Chromophores Generates the Waterâ€Resistant Nitrate Nonlinear Optical Material Bi <sub>3</sub> TeO <sub>6</sub> OH(NO <sub>3</sub> ) <sub>2</sub> . Angewandte Chemie, 2017, 129, 555-559.	2.0	12
279	A tubular luminescent framework: precise decoding of nitroaniline isomers and quantitative detection of traces of benzaldehyde in benzyl alcohol. Journal of Materials Chemistry C, 2020, 8, 9828-9835.	5.5	12
280	Realization of Inâ€Plane Polarized Light Detection Based on Bulk Photovoltaic Effect in A Polar Van Der Waals Crystal. Small, 2022, 18, e2200011.	10.0	12
281	Selfâ€Healing, Waterâ€Retaining, Antifreeze, Conductive PVA/PAAâ€PAMâ€ŀS/GC Composite Hydrogels for Strain and Temperature Sensors. Macromolecular Materials and Engineering, 2022, 307, .	3.6	12
282	Inorganicâ <sup>~*</sup> Organic Hybrid Polymersvia Hydrothermal Syntheses: Tetraaquahexakis(pyrazine-2-carboxylato)pentacopper(4+) Hexacosaoxooctamolybdate(4â^*) Polymer ({[Cu5(pzca)6(H2O)4][Mo8O26]}n; pzca=Pyrazine-2-carboxylate) and Dicopperdecaoxo(pyrazine)trimolybdenum Polymer ([Mo3Cu2O10(pz)]n; pz=pyrazine). Helvetica Chimica	1.6	11
283	Acta, 2001, 84, 3393-3402. Inclusion of Metal Complexes into Cavities of 2D Coordination Networks Built fromp-Sulfonatothiacalix[4]arene Tetranuclear Clusters. European Journal of Inorganic Chemistry, 2006, 2006, 526-530.	2.0	11
284	Two microporous metal–organic frameworks constructed from trinuclear cobalt( <scp>ii</scp> ) and cadmium( <scp>ii</scp> ) cluster subunits. CrystEngComm, 2016, 18, 2239-2243.	2.6	11
285	A Deepâ€UV Nonlinear Optical Borosulfate with Incommensurate Modulations. Angewandte Chemie, 2021, 133, 11558-11564.	2.0	11
286	Stable Fluorinated Hybrid Microporous Material for the Efficient Separation of C <sub>2</sub> –C <sub>3</sub> Alkyne/Alkene Mixtures. Inorganic Chemistry, 2022, 61, 7530-7536.	4.0	11
287	Inclusion of <i>p</i> â€sulfonatothiacalix[4]arene and its metal complexes. Chemical Record, 2009, 9, 155-168.	5.8	10
288	Precursory disilver(I) macrocycle with pendent binding sites: a new building block for targeting coordination polymers based on solvent-controlled conformational variation. CrystEngComm, 2009, 11, 576.	2.6	10

#	Article	IF	CITATIONS
289	Structural evolution via modifying (6,3) layer: from inclined polycatenation to parallel polyrotaxane-like interpenetration. CrystEngComm, 2013, 15, 8426.	2.6	10
290	Local-structure-dependent luminescence in lanthanide-doped inorganic nanocrystals for biological applications. Chemical Communications, 2021, 57, 2970-2981.	4.1	10
291	Combinatorial Selfâ€Assembly of Coordination Cages with Systematically Fineâ€Tuned Cavities for Efficient Coâ€Encapsulation and Catalysis. Angewandte Chemie, 2022, 134, .	2.0	10
292	Two Coordination Networks Built from <i>p</i> ‣ulfonatothiacalix[4]arene Tetranuclear Clusters. Zeitschrift Fur Anorganische Und Allgemeine Chemie, 2009, 635, 1669-1672.	1.2	9
293	Flexible Microporous Framework Based on Pb <sub>4</sub> Clusters for Highly Selective Storage and Separation of Energy Gases. Crystal Growth and Design, 2019, 19, 3103-3108.	3.0	9
294	A Novel Open-Framework Gallium Phosphate Containing Two Different Building Units. European Journal of Inorganic Chemistry, 2003, 2003, 1303-1305.	2.0	7
295	Linear oxalato- and 4,4â€2-dipyridyldisulfide-bridged copper(II) coordination polymer involving in situ ligand synthesis. Journal of Coordination Chemistry, 2007, 60, 2527-2532.	2.2	7
296	Extending the Structures of the <i>p</i> -Sulfonatothiacalix[4]arene Dimers Through Second-sphere Coordination and π…π Stacking Interactions. Supramolecular Chemistry, 2008, 20, 289-293.	1.2	7
297	Effects of Temperature and Anion on the Copper(II) Complexes based on 2â€ <del>(</del> Carboxyphenyl)iminodiacetic Acid and 1,10â€Phenanthroline. Zeitschrift Fur Anorganische Und Allgemeine Chemie, 2015, 641, 1998-2004.	1.2	7
298	Tuning the Structure of Fe-Tetracarboxylate Frameworks Through Linker-Symmetry Reduction. CCS Chemistry, 2021, 3, 1701-1709.	7.8	7
299	Pushing KTiOPO <sub>4</sub> -like Nonlinear Optical Sulfates into the Deep-Ultraviolet Spectral Region. Inorganic Chemistry, 2021, 60, 18950-18956.	4.0	7
300	A singleâ€structured LuAG:Ce,Mn phosphor ceramics with high CRI for highâ€power white LEDs. Journal of the American Ceramic Society, 2022, 105, 5738-5750.	3.8	7
301	Reaction of sulfur-containing structural units of transition metals. Science in China Series B: Chemistry, 1997, 40, 634-642.	0.8	6
302	Synthetic and structural chemistry of nickel(II) complexes containing dithiolato and phosphine ligands I. Preparation and crystal structure of Ni <sub>2</sub> (PPh3) <sub>2</sub> (edt) <sub>2</sub> . Chinese Journal of Chemistry, 1992, 10, 227-231.	4.9	6
303	Synthesis and Crystal Structure of a Puckered Rhombus Gridâ€like Coordination Polymer with Bridging Ligand Containing Sulfanyl Linker. Chinese Journal of Chemistry, 2004, 22, 51-54.	4.9	6
304	Pillar-Assisted Construction of a Three-Dimensional Framework from a Two-Dimensional Bilayer Based on a Zn/Cd Heterometal Cluster: Pore Tuning and Gas Adsorption. Crystal Growth and Design, 2018, 18, 1826-1833.	3.0	6
305	Controllable Coordination Selfâ€Assembly Based on Flexibility of Ligands: Synthesis of Supramolecular Assemblies and Stimuliâ€Đriven Structural Transformations. Israel Journal of Chemistry, 2019, 59, 140-150.	2.3	6
306	The partition principles for atomic-scale structures and their physical properties: application to the nonlinear optical crystal material KBe <sub>2</sub> BO <sub>3</sub> F <sub>2</sub> . Physical Chemistry Chemical Physics, 2020, 22, 19299-19306.	2.8	6

#	Article	IF	CITATIONS
307	A Hybrid Halide Perovskite Birefringent Crystal. Angewandte Chemie, 2022, 134, .	2.0	6
308	A copper(I) thiolate coordination polymer with thermochromic and mechanochromic luminescence. Inorganic Chemistry Communication, 2022, 140, 109432.	3.9	6
309	Hydrothermal Synthesis and Structures of Two One-Dimensional Heteropolytungstates Chains Formed by Keggin Cluster Units. Journal of Cluster Science, 2008, 19, 591-600.	3.3	5
310	Vanadium(IV) dimer complexes containing [V( <i>o</i> <sub>6</sub> H <sub>4</sub> OS) <sub>3</sub> ] <sup>2â^'</sup> fragment and caged sodium ions. Chinese Journal of Chemistry, 1993, 11, 30-39.	4.9	5
311	A bi-butterfly W-Cu-S cluster compound: Synthesis and crystal structure of (n-Bu4N)2[W2Cu4S8(S2CNC4H8)2]. Chinese Journal of Chemistry, 2010, 11, 144-150.	4.9	5
312	A Novel Selfâ€Penetrated Framework with New Topology Based on Rigid Ligands. Chinese Journal of Chemistry, 2014, 32, 1029-1032.	4.9	5
313	Simultaneous fluorescence and phosphorescence in Zn( <scp>ii</scp> )–zwitterionic coordination polymers with tunable colors. Journal of Materials Chemistry C, 2021, 9, 4233-4239.	5.5	5
314	A p-Sulfonatothiacalix[4]arene Supramolecular Capsule Containing a Dinuclear Copper(II) Complex. Supramolecular Chemistry, 2007, 19, 411-417.	1.2	4
315	An Uncommon Hypervalent Fluorooxosilicophosphate. Chemistry - an Asian Journal, 2019, 14, 4174-4178.	3.3	4
316	A flexible Zr-MOF with dual stimulus responses to temperature and guest molecules. Inorganic Chemistry Communication, 2021, 128, 108597.	3.9	4
317	High partial thermal conductivity of luminescence sites: a crucial factor for reducing the heat-induced lowering of the luminescence efficiency. Journal of Materials Chemistry C, 2021, 9, 14439-14443.	5.5	4
318	Whiteâ€Light Emission and Circularly Polarized Luminescence from a Chiral Copper(I) Coordination Polymer through Symmetryâ€Breaking Crystallization. Angewandte Chemie, 2022, 134, .	2.0	4
319	Fabricating ultralow-power-excitable lanthanide-doped inorganic nanoparticles with anomalous thermo-enhanced photoluminescence behavior. Science China Materials, 2022, 65, 2793-2801.	6.3	4
320	Synthesis, Structure and Magnetic Properties of a Cyclic Heterotetranuclear Co3Fe Complex of 2-Mercaptophenol (H2mp) with tri-n-Butylphosphine Participation. Journal of the Chinese Chemical Society, 1998, 45, 367-373.	1.4	3
321	Synthesis and Crystal Structures of Two Nest-Shaped Cluster Compounds, [MoOS <sub>3</sub> Cu <sub>3</sub> (SCN)py <sub>5</sub> ] and [WOS <sub>3</sub> Cu <sub>3</sub> (SCN)py <sub>5</sub> ]. Synthesis and Reactivity in Inorganic, Metal Organic, and Nano Metal Chemistry, 2000, 30, 761-775.	1.8	3
322	Synthesis, X-ray crystal structure, and magnetic property of a 3-D self-assembled supermolecule. Journal of Coordination Chemistry, 2009, 62, 2307-2315.	2.2	3
323	Solventâ€Induced Pseudopolymorphism of a New Dinuclear Oxovanadium(V) Compound Based on 2,6â€Di(hydroxymethyl)â€4â€methylphenol. Zeitschrift Fur Anorganische Und Allgemeine Chemie, 2009, 635, 379-383.	1.2	3
324	Synthesis and Crystal Structure of a Novel Hydrogenâ€Bonded Threeâ€Dimensional Polymer [Zn (1,4â€benzenedicarboxylate) â€(pyridine)ÂH <sub>2</sub> 0] <i><sub>n</sub></i> . Chinese Journal of Chemistry, 2002, 20, 1124-1128.	4.9	3

#	Article	IF	CITATIONS
325	Conformation Improving Construction of Ag3L2 Metallocages and Their Selective Encapsulation. Crystal Growth and Design, 2016, 16, 3569-3572.	3.0	3
326	An optoelectronic duple bistable phosphate with ultrahigh thermal stability. Journal of Materials Chemistry C, 2018, 6, 388-392.	5.5	3
327	Exploring the surface-to-volume ratio in ultrasmall nanocrystals using the optical probe of Eu <sup>3+</sup> ion. Chemical Communications, 2020, 56, 14725-14728.	4.1	3
328	Activating Surface Dark Emitters in Lanthanide-Doped Ultrasmall Nanoparticles for Biological Applications Based on Interparticle Energy Transfer. CCS Chemistry, 2021, 3, 2155-2163.	7.8	3
329	A flexible microporous framework with temperature-dependent gate-opening behaviours for C2 gases. Chemical Communications, 2021, 57, 3785-3788.	4.1	3
330	Lanthanide-based NIR-II Fluorescent Nanoprobes and Their Biomedical Applications <sup>※</sup> . Acta Chimica Sinica, 2022, 80, 542.	1.4	3
331	Crystal and Molecular Structure of the Copper(I)-thiolate-selenide Complex [Ph <sub>4</sub> P][Cu(SeS <sub>2</sub> CNC <sub>4</sub> H <sub>8</sub> )(S <sub>2</sub> CN <sub>2</sub> with an Unusual Se-S Bond. Zeitschrift Fur Naturforschung - Section B Journal of Chemical Sciences, 1999, 54, 1313-1317.	C <sub>4 0.7</sub>	H <sub< td=""></sub<>
332	A cobalt-selenium cluster with triethylphosphine: preparation and structure of Co6(μ3-Se)8(PEt3)6·THF. Chinese Journal of Chemistry, 2010, 9, 421-424.	4.9	2
333	Study on polyurethaneâ€acrylate/cerium dioxide modified by 3â€{Methylacryloxyl)propyltrimethoxy silane and its UV absorption property. Journal of Applied Polymer Science, 2021, 138, 50760.	2.6	2
334	A Cage-based Porous Metal-organic Framework for Efficient C2H2 Storage and Separation. Chemical Research in Chinese Universities, 2022, 38, 82-86.	2.6	2
335	Adaptive coordination assemblies based on a flexible tetraazacyclododecane ligand for promoting carbon dioxide fixation. Chemical Science, 2022, 13, 9016-9022.	7.4	2
336	Synthesis and structure of a novel MoFe4S4 cubane-like cluster (Me3PhCH2N)2 [MoFe4S4 (SC6H11)7]. Science in China Series B: Chemistry, 1998, 41, 301-308.	0.8	1
337	SYNTHESES AND STRUCTURES OF CLUSTER COMPOUNDS CONTAINING WSe <sub>4</sub> Cu <i>n</i> ( <i>n</i> = 3,4) CORES WITH DIALKYLDITHIOCARBAMATE LIGANDS. Journal of Coordination Chemistry, 2000, 49, 227-238.	2.2	1
338	Synthetic and structural chemistry of hexacobalt cluster compounds II. Preparation and structure of Co6(1¼-S)8 (Ph2PCH2P(O)Ph2)6. Chinese Journal of Chemistry, 2010, 9, 425-429.	4.9	1
339	Synthesis, structure, magnetic property and selective dye absorption of a coordination polymer with intrinsic positive charged sites. Inorganic Chemistry Communication, 2021, 123, 108323.	3.9	1
340	Study on a novel fluorescent anti-counterfeiting acrylate pressure-sensitive adhesive. Journal of Adhesion, 2022, 98, 1151-1167.	3.0	1
341	A red-emissive 3D framework with the coexistence of copper-iodide clusters and rings as a luminescent ratiometric thermometer. Inorganic Chemistry Communication, 2021, 127, 108517.	3.9	1
342	In Honor of Professor Xintao Wu on the Occasion of His Eightieth Birthday. Crystal Growth and Design, 2019, 19, 5457-5459.	3.0	0

#	ARTICLE	IF	CITATIONS
343	Conformation-Driven Self-Assembly: From a 1D Metal–Organic Polymer to an Infinite Double Nanotube. ACS Omega, 2019, 4, 10755-10760.	3.5	Ο
344	Titelbild: Electricâ€Field Assisted Inâ€Situ Hydrolysis of Bulk Metal–Organic Frameworks (MOFs) into Ultrathin Metal Oxyhydroxide Nanosheets for Efficient Oxygen Evolution (Angew. Chem. 31/2020). Angewandte Chemie, 2020, 132, 12645-12645.	2.0	0
345	Innenrücktitelbild: Induction of Chirality in a Metal–Organic Framework Built from Achiral Precursors (Angew. Chem. 6/2021). Angewandte Chemie, 2021, 133, 3351-3351.	2.0	Ο
346	Exploring a Fatigueâ€Free Layered Hybrid Perovskite Ferroelectric for Photovoltaic Nonâ€Volatile Memories. Angewandte Chemie, 2021, 133, 10692-10696.	2.0	0
347	DESIGN OF METAL-CARBOXYLATE CAVITY-CONTAINING RECTANGULAR GRIDS WITH 1,2,4,5-BENZENETETRACARBOXYLIC ACID. , 2002, , .		0
348	STRATEGIES FOR THE CONSTRUCTION OF COMPLEXES BASED ON METAL CLUSTERS. , 2002, , .		0